

## TREATMENT

UDC 621.771.013:620.186:620.172.2

### STRUCTURAL CHANGES IN STEEL 12GBA DURING WARM ROLLING AND RESISTANCE TO BRITTLE FRACTURE AT NEGATIVE TEMPERATURES

L. S. Derevyagina,<sup>1</sup> A. V. Korznikov,<sup>2</sup> N. S. Surikova,<sup>1</sup> and A. I. Gordienko<sup>1</sup>Translated from *Metallovedenie i Termicheskaya Obrabotka Metallov*, No. 11, pp. 48 – 55, November, 2017.

---

The effect of warm rolling (at 750 – 550°C) on the structure and mechanical properties of low-carbon steel 12GBA is studied in tensile tests in a wide temperature range. Metallographic analysis with the use of optical, scanning electron and transmission electron microscopy is performed. The strength and ductility properties are determined in tensile tests at from 20°C to –196°C. The suggested mode of warm rolling is shown to affect favorably the structure and the combination of mechanical properties of steel 12GBA.

---

**Key words:** warm rolling, low-carbon steel, cementite morphology, texture, strength, ductility, micromechanisms of fracture.

#### INTRODUCTION

The strength of structures from cold-brittle steels is commonly elevated by increasing the specific amount of metal per structure, which causes overconsumption of metal. The demand for cold-brittle steels is growing due to fast development of Northern territories. In this connection, the quality standards involve lowering of the metal intensity of structures. Solution of the problem requires detailed information on the interrelation between the mechanical properties and the macro- and microstructures of steels. The physical side of the phenomenon of failure of structures is also important, because reduction of the consumption of metals in an article and increase in the level of active stresses elevates the danger of their early failure. The metal intensity of structures can be lowered by raising the strength of the steels by methods of severe plastic deformation. As a result of such treatment, the sizes of the components of the grain and subgrain structures are decreased and the strength of the steel is increased. Its strength and plasticity properties also affect the grain boundaries due to their great length and nonequilibrium condition and some other factors.

The effect of uniform isothermal forging (UIF) on the structure, mechanical properties and fracture behavior of pipe steel 12GBA has been studied in [1, 2]. It has been shown that the forging treatment of steel 12GBA promotes formation of an ultrafine-grained structure and substantial increase in the mechanical properties. However, the presence of a cubic texture component causes brittle cleavage and lowers the fracture toughness in the temperature range from room one to –40°C. After the forging treatment, the impact toughness of the steel at a temperature below –40°C exceeds somewhat the value in the initial (coarse-grained) condition [2].

The aim of the present work was to study the regular features of variation of structure in low-carbon pipe steel 12GBA after warm rolling and to estimate its effect on the mechanical properties and on the fracture behavior under the conditions of static tension at negative temperatures.

#### METHODS OF STUDY

We studied steel 12GBA of the following chemical composition (in wt.%): 0.11 C, 1.2 Mn, 0.25 Si, 0.05 Nb, 0.35 Cu, 0.0026 Al, 0.005 S, 0.0012 P.

Ingot from steel 12GBA with typical ferrite-pearlite structure were rolled in several passes with step lowering of the temperature. The rolling was started in the intercritical temperature range at 750°C and finished in the ferritic range

---

<sup>1</sup> Institute of Strength Physics and Materials Science of the Siberian Branch of the Russian Academy of Sciences, Tomsk, Russia (e-mail: lsd@ispms.tsc.ru).

<sup>2</sup> Institute for Problems of Superplasticity of Metals of the Russian Academy of Sciences, Ufa, Russia.

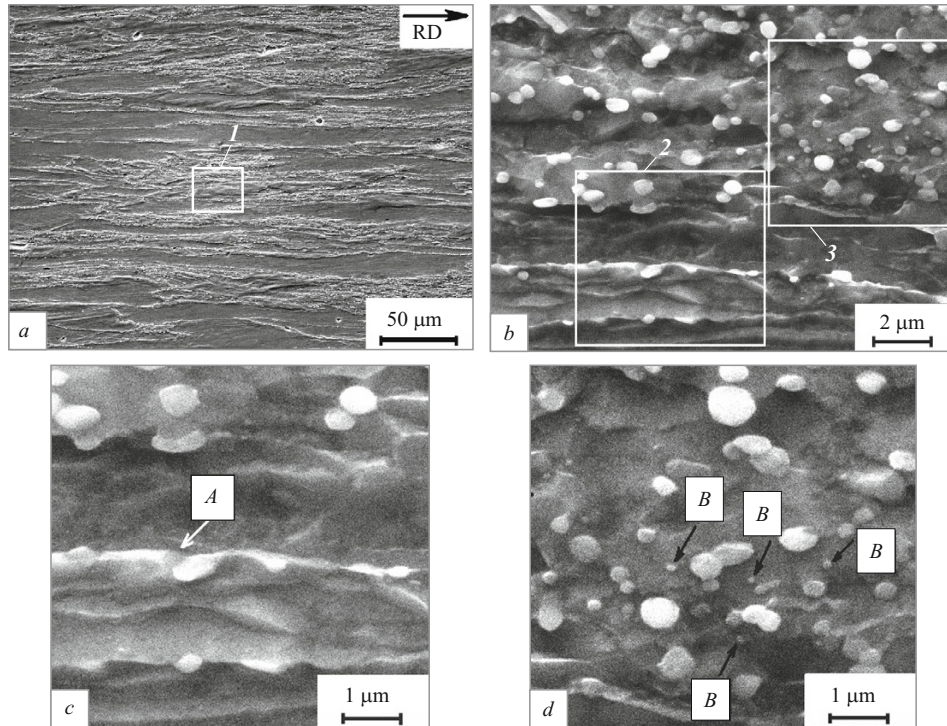


**Fig. 1.** Microstructure of steel 12GBA after warm rolling (*a*) and its region (*b–d*) at higher magnifications (SEM): *b*) region 1; *c, d*) regions 2 and 3, respectively; *A*) crushing of a carbide plate; *B*) globular carbides.

at 550°C. This temperature range was chosen with the aim to obtain the highest strengthening of the steel due to growth in the dislocation density and to create a branched substructure in order to make the process of precipitation hardening during the rolling easier. The rolling was conducted on sizing rolls with rectangular-section passes with contraction  $\psi = 10 - 15\%$  in each pass to a final bar section of  $10 \times 10$  mm. The total rolling strain  $\varphi = 2.7$ , which is almost twice lower than under UIF ( $\varphi = 6.2$ ) [2].

The structure was studied under a Zeiss Axiovert 25 optical microscope and a Philips SEM 515 scanning electron microscope in the mode of secondary electrons. To study the morphological features of the structure and to plot the maps of phase distribution we used a Quanta 200 3D scanning electron microscope in the mode of back-scattered electrons (EBSD). To determine the structure at the microscale level we studied foils under a SM-12 transmission electron microscope. The phase composition of the steel was analyzed by indexing the electron diffraction patterns. The phases were identified by analyzing dark-background images.

To evaluate the mechanical properties, we conducted tensile tests of specimens shaped as a double blade with functional part  $15 \times 3 \times 1$  mm in size at a temperature ranging from +20 to  $-196^\circ\text{C}$ . The results of the tests were used to plot the temperature dependences of the strength and ductility characteristics, i.e., the yield strength  $\sigma_{0.2}$ , the ultimate strength  $\sigma_r$ , the uniform strain  $\delta_u$ , and the total strain  $\delta_{tot}$ .

The fracture micromechanisms required for qualitative estimation of the fracture toughness of the steel were studied by the method of scanning electron microscopy (SEM).

## RESULTS

### Structure of the Steel after Warm Rolling

The SEM studies of the structure have shown that after the warm rolling it is represented by a mixture of ferrite grains strained and elongated in the direction of the deformation and globular (granular) pearlite (Fig. 1*a*).

The EBSD maps of the grain structure have shown that the mean effective size of ferrite grains in the section orthogonal to the rolling direction (see Fig. 2*a* and *b*)  $d = 2.43 \mu\text{m}$ . The grain size was understood as the diameter of a circle with an area equal to the area of the grain on the lap. It can be seen from Fig. 2*c* that the dominant place of location of particles of the tertiary carbide of a micron size are pearlite regions and grain boundaries of the free ferrite.

The curve describing the grain size distribution has a lognormal form with left asymmetry, which indicates substantial grain size heterogeneity in the steel after the treatment.

After warm rolling, the total density of grain boundaries in the structure of the steel increased by a factor of 8 as compared to the initial value (Table 1). The proportion of the density of the low-angle grain boundaries (LAB) to that of

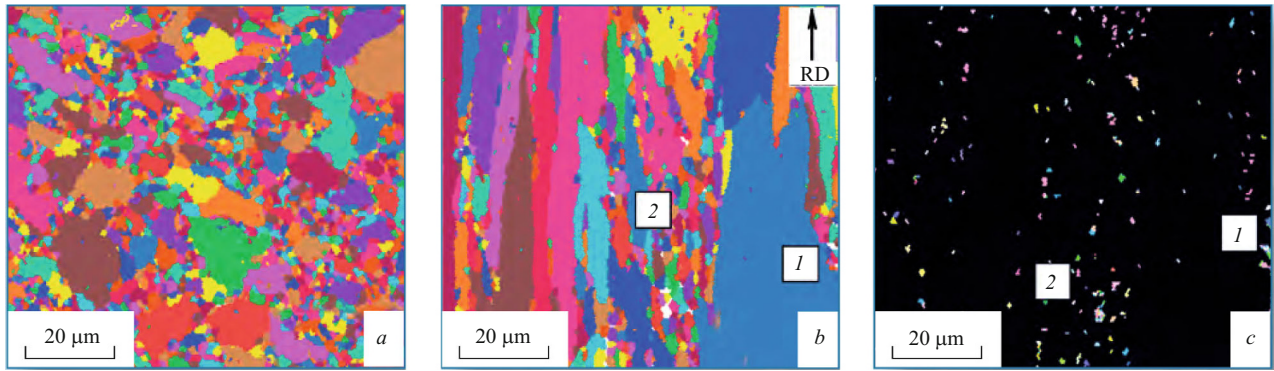


**Fig. 2.** EBSD maps of steel 12GBA after warm rolling in transverse (*a*) and longitudinal (*b*, *c*) sections: *a*, *b*) grain structure of  $\alpha$ -phase; *c*)  $\text{Fe}_3\text{C}$  carbide; 1) ferrite grain; 2) pearlite grain.

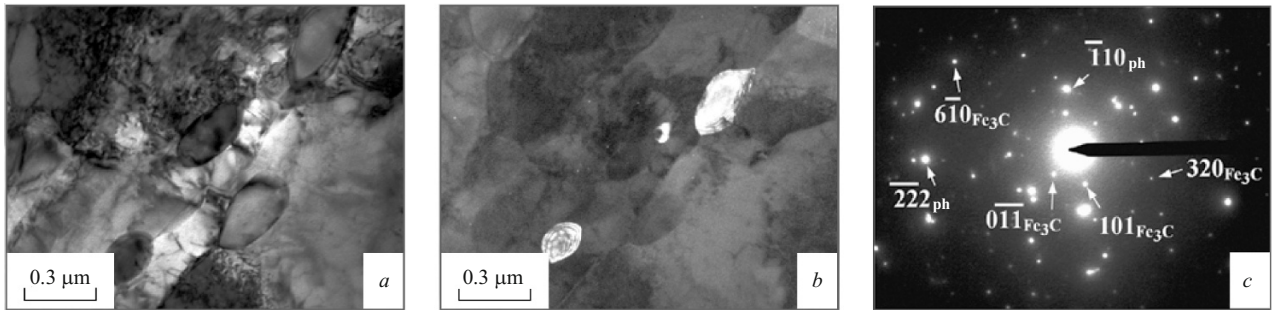


**Fig. 3.** Lenticular particles of cementite in steel 12GBA on grain boundaries and close to them: *a*) light-background field; *b*) dark-background field in reflection 101 of cementite; *c*) microdiffraction pattern (zone [112] of ferrite, zones [2] and [6] of  $\text{Fe}_3\text{C}$  cementite).

the high-angle boundaries (HAB) changed in the rolled steel chiefly due to the growth of the fraction of LAB. For example, the density of HAB and LAB in the initial fine-grained structure was 90 and 10%, respectively. After the warm rolling, the density of HAB decreased to 45% and that of LAB increased to 55% of the total density of the boundaries (Table 1).

After UIF [2], the density of HAB in the structure decreased to about 24%, and the density of LAB increased to about 76%. With growth of the total strain the angles  $\varphi$  of the off-orientation of LAB grew (to 200), i.e., the LAB were gradually transformed into HAB.

The electron-microscope study has shown that the ferrite grains in steel 12GBA after warm rolling have a banded structure with a mean size of the fragments about 0.2 – 0.5  $\mu\text{m}$  in the direction orthogonal to the rolling one. Lenticular particles of  $\text{Fe}_3\text{C}$  cementite 150 – 500 nm in size are arranged at the junctions of several grains and in the region of grain and subgrain boundaries (see Fig. 3). These data confirm the results of the study of the microstructure of the rolled steel by the EBSD method, optical and scanning electron microscopy (Figs. 1*b* and 2*c*). The structure of the steel also contains precipitates of fine particles of  $\text{Fe}_2\text{C}$   $\varepsilon$ -carbide with hexagonal lattice and a mean size  $d_0 = 12$  nm,  $\text{Nb}_2\text{C}$

carbide with  $d_0 = 5 - 8$  nm (Fig. 4), and coarse particles of  $\text{Mn}_7\text{C}_3$  and  $\text{Mn}_{23}\text{C}_6$  carbides ( $d_0 \sim 30 - 500$  nm). They are located both over grain and subgrain boundaries and in the volume of the ferrite phase.

We observed precipitates of a cementite phase in the form of stretched layers about 100 nm wide over grain boundaries of steel 12GBA with coarse-grained structure as a well as fine ( $d_0 \sim 20$  nm) particles of  $\text{Fe}_3\text{C}$  carbide in the bulk of grains and on subgrain boundaries.

By the data of the electron microscope studies, dislocation micromechanisms of plastic flow act in steel 12GBA under tensile tests conducted in the temperature range from

**TABLE 1.** Structural Characteristics of Steel 12GBA

Structural state	$d$ , $\mu\text{m}$	$\rho$ , 1/ $\mu\text{m}$	Density	
			HAB	LAB
Coarse-grained	25.00	0.17	89.0	11.0
After warm rolling	2.47	1.36	45.4	54.6
After UIF [2]	0.57	2.25	24.4	75.6

**Notations:** UIF) uniform isothermal forging;  $d$ ) mean grain size;  $\rho$ ) density of all grain boundaries; HAB and LAB) high-angle and low-angle grain boundaries, respectively.



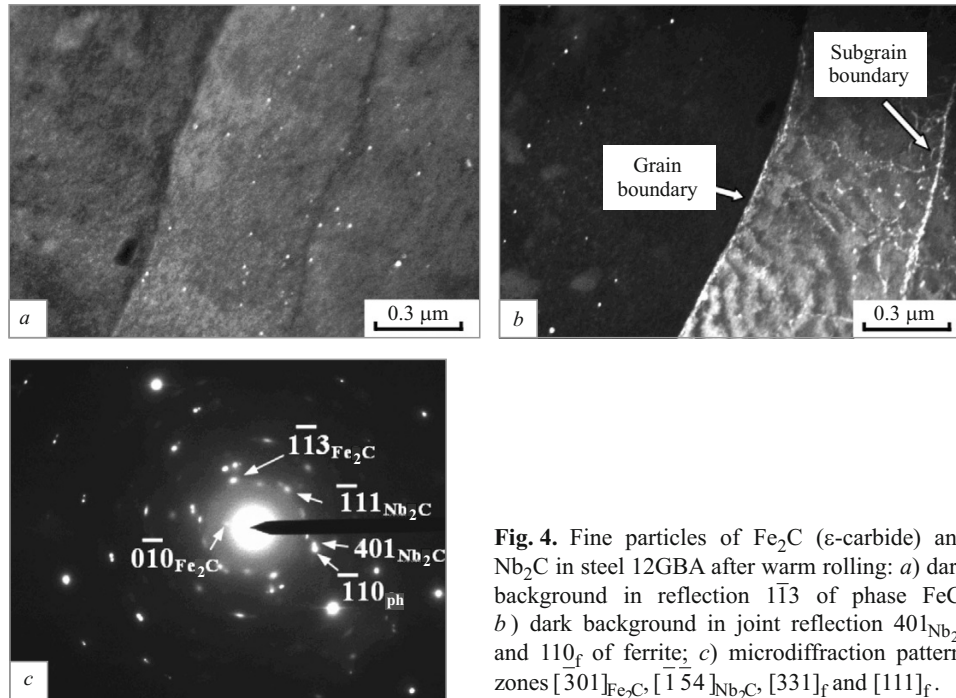


**Fig. 4.** Fine particles of  $\text{Fe}_2\text{C}$  ( $\epsilon$ -carbide) and  $\text{Nb}_2\text{C}$  in steel 12GBA after warm rolling: *a*) dark background in reflection  $\bar{1}\bar{1}3$  of phase  $\text{FeC}$ ; *b*) dark background in joint reflection  $401_{\text{Nb}_2\text{C}}$  and  $110_{\text{f}}$  of ferrite; *c*) microdiffraction pattern, zones  $[301]_{\text{Fe}_2\text{C}}$ ,  $[\bar{1}\bar{1}54]_{\text{Nb}_2\text{C}}$ ,  $[331]_{\text{f}}$  and  $[111]_{\text{f}}$ .

+20°C to -196°C. A twinning micromechanism of plastic flow in the range of negative temperatures, which determines the strong temperature dependence of the yield strength in bcc materials, has not been detected.

The initial structural state with coarse grains in steel 12GBA was virtually textureless, which is typical for finish rolling of the steel in the temperature range of recrystallized austenite (1100 – 950°C).

Figure 5 presents direct and inverse pole figures of rolled bars from steel 12GBA. Analysis of the pole figures has

shown that the central layers in the rolling plane contain orientations of crystallographic planes  $\{111\}$  and  $\{554\}$  (Fig. 5*a* and *b*), and the rolling direction coincides with direction  $\langle 110 \rangle$  (Fig. 5*c*).

The textures forming under deformation and heat treatment of low-carbon steels have been studied in [3 – 7]. Texture components form in competing processes such as straining, dynamic and static recrystallization of  $\gamma$ - and  $\alpha$ -phases, and  $\gamma - \alpha$  phase transformation of the textures  $\gamma$ -phase. As a consequence, an inhomogeneous multicomponent texture is

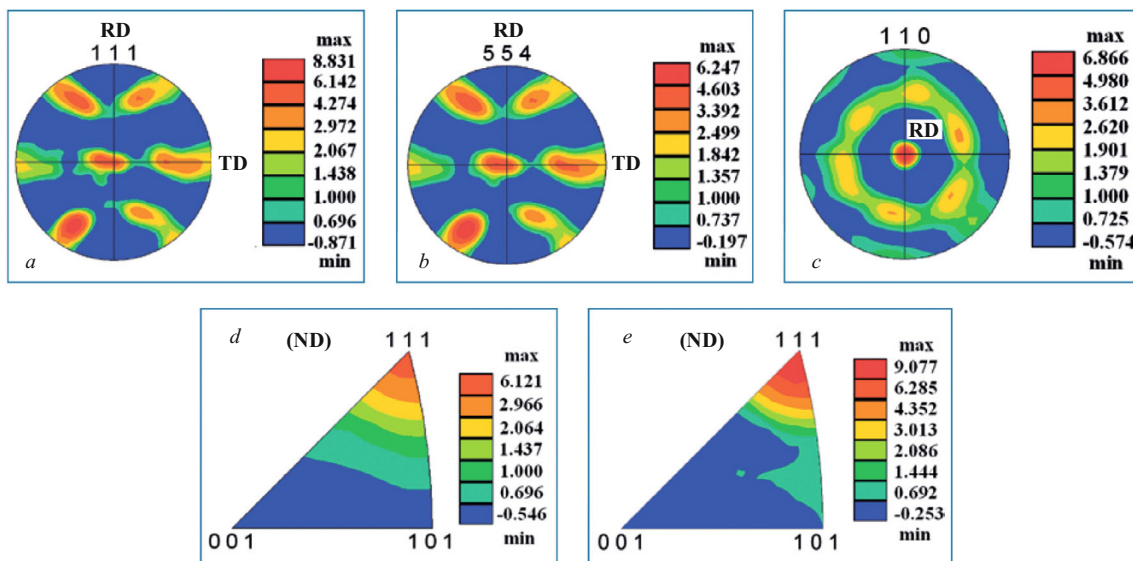


**Fig. 5.** Direct (*a* – *c*) and inverse (*d*, *e*) pole figures of rolled steel 12GBA obtained in the rolling plane (*a*, *b*, *d*, *e*) and in a plane orthogonal to the rolling direction (*c*): ND) normal to the rolling direction; RD) rolling direction; TD) normal to RD and ND passing in the rolling plane; *a* – *d*) at 20°C; *e*) at -80°C.

**TABLE 2.** Mechanical Characteristics of Steel 12GBA at Room Temperature

Structural state	$\sigma_{0.2}$ , MPa	$\sigma_r$ , MPa	$\sigma_{0.2}/\sigma_r$	$\delta_u$ , %	$\delta_{tot}$ , %
Coarse-grained	310	580	0.53	24.00	27.0
After warm rolling	600	695 – 780	0.86 – 0.77	9.53	16.4
After UIF [2]	880	930	0.95	~ 0.50	1.0

commonly observed over cross section of the sheet. It has been shown that deformation of materials with bcc lattice yields a texture in which the directions of axes  $\langle 110 \rangle$ ,  $\langle 112 \rangle$  coincide with the rolling direction, and the rolling plane contains orientations passing over the edge of the stereographic triangle  $\{001\}$ - $\{111\}$ . The strain-induced textures coincide with the recrystallization texture  $\{001\}\langle 100 \rangle$  of the  $\alpha$ -phase, and the surface layers of the rolled sheet contain shear (friction) textures  $\{110\}\langle 001 \rangle$ .

Crystallographic texture  $\{111\}\langle 110 \rangle$  detected in the present work corresponds to the plane strain texture of the  $\alpha$ -phase and does not contradict the data reported in [3 – 7]. The forming texture is characterized by considerable scattering (Fig. 5d). In the opinion of the authors of [6], a texture component  $\{554\}\langle 225 \rangle$  close to  $\{111\}\langle 110 \rangle$  forms due to the texture of the  $\gamma - \alpha$  transformation developing without load. Indeed, the rolling plane exhibits crystallites with orientation  $\{554\}$  (Fig. 5b) with pole density of component  $P^{(554)}(\gamma - \alpha) = 6.2$ , which is comparable to the value of  $P_{\alpha}^{(111)} = 6.14$ . Thus, it can be assumed that the scattering of texture  $\{111\}\langle 110 \rangle$  (Fig. 5d) may affect the  $\gamma - \alpha$  phase transformation.

If the specimens of the rolled steel are subjected additionally to tension under a negative temperature, the texture is not only preserved, but becomes more perfect (Fig. 5d). For example, the pole density of texture component  $\{111\}\langle 110 \rangle$  reached  $P_1^{111} \sim 6$  in a specimen after rolling, while an additional tension at  $-80^\circ\text{C}$  raised the  $P_2^{111}$  to about 9 (Fig. 5d). This inference agrees with the opinion of the author of [3] who states that the sharpness and perfection of texture components increase with decrease of the deformation temperature.

### Mechanical Properties of Steel 12GBA

According to the results of the tensile tests at room temperature, the refinement of the structure due to rolling almost doubles the yield strength  $\sigma_{0.2}$  of the alloy (from 310 to 600 MPa) and increases the ultimate strength  $\sigma_r$  by about 39% (from 580 MPa in the coarse-grained condition to 740 MPa) (Table 2). The growth in the strength characteristics is accompanied by decrease in the plasticity by about 40%. When the temperature is decreased from room one to  $-80^\circ\text{C}$ , the strength and plasticity characteristics of the treated steel change inconsiderably but their scattering is substantial (Fig. 6). With lowering of the temperature to that

of liquid nitrogen, the strength properties of the rolled steel increase by about 50% and the plasticity properties decrease by about 20%.

In the steel with an initially coarse-grained structure in the temperature range from  $-80$  to  $-196^\circ\text{C}$  the dependence of the strength properties on the temperature is stronger than in the steel with refined structure. For example, the strength characteristics at the temperature of liquid nitrogen increase by a factor of 2 – 2.5, which is higher than the same characteristics of the steel after warm rolling (Fig. 6a) at about 30% decrease in the plasticity.

### Micromechanisms of Fracture of Steel 12GBA under Tension at Negative Temperatures

Practical application of pipe steels at negative temperatures requires high fracture toughness in addition to a high

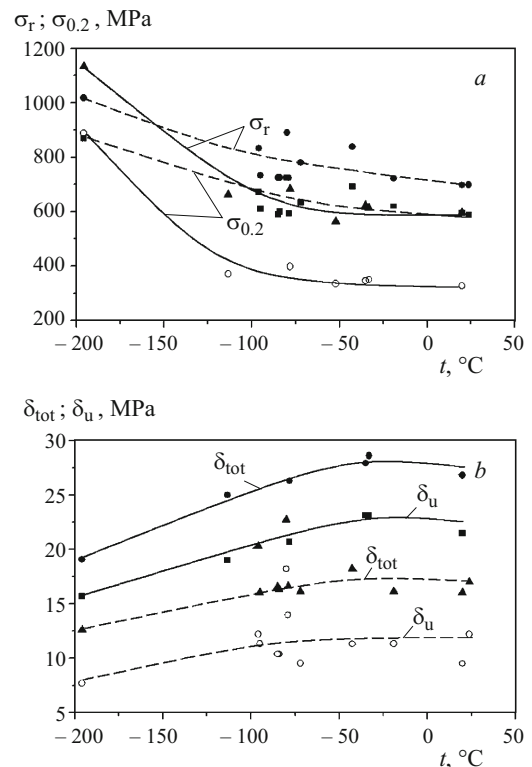


**Fig. 6.** Temperature dependences of mechanical characteristics of steel 12GBA: a) yield strength  $\sigma_{0.2}$  and ultimate strength  $\sigma_r$ ; b) uniform elongation  $\delta_u$  and total elongation  $\delta_{tot}$ ; the solid lines are used for the coarse-grained (initial) state; the dashed lines are used for the state after warm rolling.

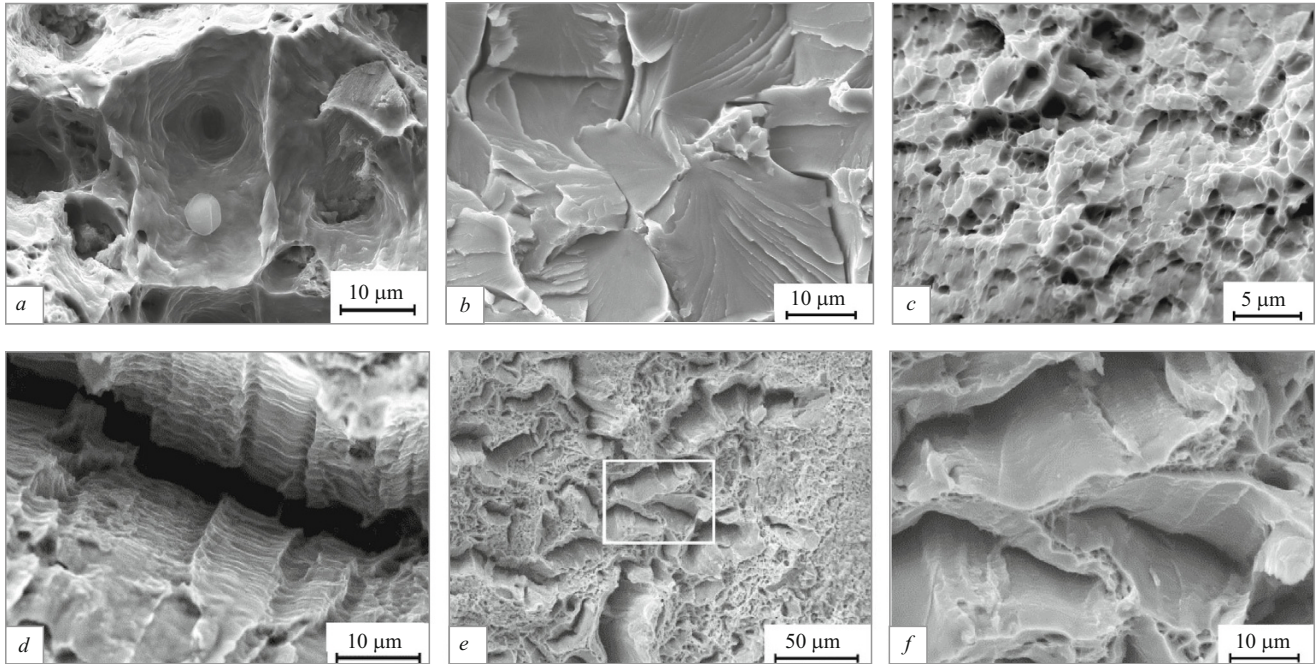


**Fig. 7.** Fracture surfaces of steel 12GBA in coarse-grained state (*a, b*) and after warm rolling (*c–f*) at different test temperatures: *a, c*) at room temperature; *d*) at  $-93^{\circ}\text{C}$ ; *b, e, f*) at  $-196^{\circ}\text{C}$ ; *f*) magnified rectangular region from Fig. 7*e*.

strength. To obtain a qualitative estimate of fracture toughness of steel 12GBA we studied the micromechanisms of fracture on tensile specimens in different structural states.

The fracture surfaces of the specimens in the initial (coarse-grained) state tested for tensile strength at room temperature have a characteristic dimple pattern (Fig. 7*a*). The diameters of the cone-like dimples are about  $25\ \mu\text{m}$ , which is comparable to the mean grain size. With increase of the negative temperatures the micromechanism of ductile dimple fracture is preserved, but the density and the depth of the dimples decrease; smooth laminated areas and small cracks with river-line pattern on their banks appear. At the temperature of liquid nitrogen, the ductile (dimple) micromechanism of fracture is replaced by transcrystalline brittle cleavage with typical cleavage facets and river-line pattern on them over the whole of the fractured area (Fig. 7*b*).

Specimens of steel 12GBA after warm rolling and tensile testing until failure at room temperature have ductile fractures (Fig. 7*c*). The  $2\text{--}5\text{-}\mu\text{m}$  size of the dimples corresponds to the mean grain size. With decrease of the test temperature the fractures acquire first short and then long and widely opened cracks (Fig. 7*d*). The walls of the cracks are covered with periodically arranged slip steps similar to those observed on the front and side faces of a broken specimen in the region of the neck. At  $-196^{\circ}\text{C}$ , the density of cracks in the fracture increases considerably (Fig. 7*e*). However, even at the temperature of liquid nitrogen the walls of the widely opened cracks preserve poorly noticeable slip steps indicating that the cracks have propagated by development of plastic zones in front of their tips (Fig. 7*f*).

## DISCUSSION

The changes in the structure of the rolled steel (extended ferrite and pearlite grains, refinement of the grain-subgrain structure) are typical for the temperature modes of warm rolling in the absence of recrystallization [8, 9]. The general laws of transformations of structural components in the steel after warm rolling and UIF [2] are similar, but there are qualitative differences. For example, pearlite with a lamellar form of cementite (a typical structure for the coarse-grained state and for the state after UIF) transforms during warm rolling into a granular ferrite-cementite structure (Fig. 1*b*). Changes in the shape of the carbide phase in the pearlitic zones of steels during plastic deformation have been observed by many authors [10–15]. Mechanisms of transformation of lamellar-shape carbides into a globular shape in the course of deformation have been suggested in [11, 13–15]. In the present work, the steel specimens in ferrite-pearlite condition were first heated to  $750^{\circ}\text{C}$  and then rolled with lowering the temperature to  $550^{\circ}\text{C}$ . Getting into the double-phase range under heating to  $750^{\circ}\text{C}$ , the carbides have enough time to dissolve completely, and the carbon-supersaturated  $\alpha$ -phase transfers into  $\gamma$ -phase, while in the subsequent rolling under the conditions of fast lowering of the temperature carbon precipitates from the austenite and coagulates in the form of carbide particles of a globular shape (region *B* in Fig. 1*d*). Upon further decrease of the rolling temperature, the carbon-depleted  $\gamma$ -phase undergoes a backward  $\gamma\text{--}\alpha$  transformation. If the carbide plates do not dissolve completely in the intercritical range, the rolling causes their



breakage and subsequent spheroidization (region *A* in Fig. 1c).

A principally new mechanism of dissolution of cementite plates is suggested in [15]. According to [15], interstitial bifurcation pores and new structural states arise in the process of plastic deformation on the ferrite-cementite interface in pearlitic regions in zones of local curvature of the crystal lattice. This creates conditions for diffusion of carbon atoms and dissolution of cementite plates, which results in their crushing and spheroidization.

Refinement of the structure and substructure components due to the development of the process of fragmentation under deformation elevates the strength properties of the steel due to grain-boundary and substructural hardening. The higher the total strain  $\varphi$ , the smaller the size of the structural component, the higher the total density of the boundaries, and hence the higher the strength properties of the steel. A certain contribution into the effect of multilevel precipitation hardening is made by fine  $\text{Nb}_2\text{C}$ ,  $\text{Fe}_2\text{C}$ ,  $\text{Fe}_3\text{C}$  carbide particles 5 – 12 nm in size, which precipitate under rolling in the bodies of grains of the  $\alpha$ -phase. The mechanical characteristics of the metal depend not only on the grain-boundary and precipitation hardening but also on the properties of the grain boundaries and the related stresses. Refinement of the structure and enhancement of the grain-boundary hardening are accompanied by changes in the spectrum of off-orientations of the ensemble of the boundaries. Growth of the total strain  $\varphi$  is accompanied by increase in the fraction of LAB (Table 1), which make their contribution into the multilevel strain hardening. As a result of the joint action of the mentioned hardening mechanisms, the yield strength  $\sigma_{0.2}$  of steel 12GBA after warm rolling is 1.93 times higher than in the not deformed steel.

With growth of the strength properties of the steel after warm rolling, the plasticity parameters decrease, but their level is still quite high (Table 2). On the contrary, the strain of the metal  $\varepsilon$  in the stage of uniform plastic flow in the tensile tests of the steel after UIF decreases abruptly to about 0.5%, and localized flow develops rapidly due to the high flow stresses and high fraction of LAB ( $\sigma_{0.2}/\sigma_r = 0.95$ , Table 2). After the warm rolling, the steel manifests a lower susceptibility to strain localization ( $\sigma_{0.2}/\sigma_r \sim 0.82$ , Table 2).

Analyzing the dependences of the strength and plasticity characteristics on the temperature of the steel subjected to warm rolling (Fig. 6), we detected considerable scattering of the data. In all probability, it is connected with the differences in the grain sizes of the ferrite phase. The differences in the grain sizes may be connected in their turn with the more intense crushing of the pearlite regions containing a carbide phase as compared to the grains of free ferrite under the rolling (regions 2 and 1 in Fig. 2b and c). Scattering is virtually absent on similar curves for the steel in the initial coarse-grained state (Fig. 6), because the grain size in its structure is more homogeneous.

The strength and plasticity properties of steel 12GBA with coarse-grained structure tested at a temperature below  $-80^\circ\text{C}$  depend strongly on the temperature (Fig. 6a). The appearance of regions fractured by a brittle cleavage micromechanism at  $-196^\circ\text{C}$  seems to be explainable by abrupt growth of its strength properties with decrease of the temperature and by a stringent stress state. In addition, the decrease in the fracture toughness of steel 12GBA with coarse-grained structure at low test temperatures may be caused by the presence of extended layers of brittle  $\text{Fe}_3\text{C}$  carbides over grain boundaries.

The temperature dependence of the strength and plasticity properties of the rolled steel is weak and we should not expect a radical change in the micromechanisms of fracture under the conditions of tensile deformation. With decrease of the test temperature an additional micromechanism starts to act in the form of ductile cracks opening by development of zones of plastic flow at their tips. Like in the process of formation of pores, the energy of propagation of ductile cracks is higher than in the case of formation of cleavage cracks. However, it cannot be excluded that applying more rigid modes of mechanical testing, like impact tests, we will observe purely brittle micromechanisms of cleavage fracture.

Both the mechanical properties of the material and its fracture behavior are texture-sensitive. For this reason, we should pay special attention to the effect of crystallographic texture on the fracture toughness. It has been shown in [2] that the final stage of finishing upsetting in UIF yields a double axial texture  $\langle 111 \rangle + \langle 100 \rangle$ . The presence of a cubic texture component  $\langle 100 \rangle$ , which is dangerous if the rolled steel has enhanced susceptibility to brittle fracture, causes [7] coarse foliations, brittle regions of cleavage fracture and lowering of the fracture toughness.

After warm rolling, steel 12GBA acquires a  $\{111\}\langle 110 \rangle$  rolling texture. A steel with such texture is well adaptable to pressure treatment and possesses a high capacity for hindering crack formation under operation [7]. Thus, the presence of rolling texture  $\{111\}\langle 110 \rangle$  affects positively the mechanical properties and the fracture behavior of the metal. The fracture toughness of steel 12GBA is also increased due to replacement of the lamellar shape of carbides in pearlitic regions by a globular shape [12 – 14, 16]. By the data of the comparative analysis made in [17], warm rolling provides higher values of impact fracture toughness in steel 12GBA in the range from room temperature to  $-80^\circ\text{C}$  than uniform isothermal forging.

## CONCLUSIONS

1. Warm rolling of steel 12GBA causes the following structural changes:
  - refinement of the structure to a medium value of 2.43  $\mu\text{m}$  for the effective grain size and 0.2 – 0.5  $\mu\text{m}$  for the subgrain size;

– growth of the total density of grain-subgrain boundaries by a factor of 8 and change in the spectrum of the off-orientation angles of the boundaries, as a result of which the density of the low-angle boundaries increases from 11% in the initial coarse-grained condition to about 55% after the steel is rolled;

– replacement of the lamellar morphology of the carbide phase in pearlite grains by a globular one;

– precipitation of fine carbide particles 5 – 12 nm in size on the boundaries of the grain-subgrain structure and in the bulk of the phases;

– formation strain texture  $\{111\}\langle 110 \rangle$  of  $\alpha$ -phase with a high (over 6) pole density of the texture component in the central sections of rolled bars.

The use of warm rolling and the associated structural changes make it possible to raise the general level of the strength properties of steel 12GBA (the yield strength by a factor of 2 and the ultimate strength by a factor of 1.3) as compared to the properties of the steel in the initial coarse-grained condition. The plasticity properties in this case decrease by 40% but their level is still high enough ( $\delta_u \sim 10\%$ ,  $\delta_{tot} \sim 16\%$ ).

The brittle cleavage fracture of specimens of steel 12GBA with coarse-grained structure at the temperature of liquid nitrogen may be a consequence of the rigidity of the stress state in the neck due to the strong temperature dependence of the yield stress. On the contrary, the inconsiderable effect of the temperature on the yield strength in rolled steel 12GBA preserves the ductile (energy-intensive) micromechanisms of fracture at a test temperature from +20 to  $-196^\circ\text{C}$ .

*The work has been performed with financial support of the Russian Foundation for Basic Research (project number 16-48-700257\_r-a).*

## REFERENCES

1. I. M. Safarov, A. V. Korznikov, S. N. Sergeev, et al., "Effect of submicrocrystalline condition on the strength and impact toughness of low-carbon steel 12GBA," *Fiz. Met. Metalloved.*, No. 10, 1055 – 1060 (2012).
2. L. S. Derevyagina, A. V. Korznikov, I. M. Safarov, et al., "Effect of uniform isothermal forging on the structure, mechanical properties and fracture mechanism of steel 12GBA," *Deform. Razrush. Mater.*, No. 10, 25 – 32 (2012).
3. N. P. Lyakishev, V. F. Shamray, S. Ya. Betsofen, and Yu. L. Lipikhin, "Texture and anisotropy of properties of hot-rolled steels from steels St<sub>3</sub>sp and 09G2S," *Metally*, No. 1, 122 – 126 (1993).
4. N. P. Lyakishev, V. F. Shamray, E. B. Rubina, et al., "Formation of texture in sheets from microalloyed steel 09G2S," *Metally*, No. 5, 22 – 28 (1995).
5. I. V. Egiz, A. A. Babareko, and V. F. Shamray, "About the distribution of cracks in rolled textured sheets from ferritic steel and articles from them," *Metally*, No. 6, 80 – 90 (2000).
6. I. V. Egiz and V. F. Shamray, "Design and construction of direct pole figures for textures formed under phase transformation in iron," *Metalloved. Term. Obrab. Met.*, No. 2, 9 – 12 (2001).
7. I. V. Egiz and V. F. Shamray, "Crystallographic texture as a means for controlling the process of rolling of sheets from low-carbon steel," *Metalloved. Term. Obrab. Met.*, No. 1, 33 – 36 (2003).
8. A. I. Yurkov, Yu. V. Mil'man, and A. V. Byakova, "Structure and mechanical properties of iron after surface plastic deformation by friction. 1. Special features of structure formation," *Deform. Razrush. Mater.*, No. 1, 2 – 11 (2009).
9. V. M. Schastlivtsev, T. I. Tabatchikova, I. L. Yakovleva, et al., "Effect of regimes of thermomechanical treatment on the structure and properties of rolled sheets from low-carbon low-alloy steels," *Vopr. Materialoved.*, No. 3, 13 – 23 (2005).
10. I. M. Safarov, S. N. Sergeev, R. M. Galeev, et al., "Strength and impact toughness of low-carbon steel 12GBA with fibrous UFG structure," *Fiz. Met. Metalloved.*, **115**(3), 1 – 9 (2014).
11. R. Song, D. Ponge, and D. Raabe, "Mechanical properties of an ultrafine grained C – Mn steel processed by warm deformation and annealing," *Acta Mater.*, **53**, 4881 – 4892 (2005).
12. S. M. L. Sastree, S. V. Dobatkin, and S. V. Sidorova, "Formation of submicrocrystalline structure in steel 10G<sub>2</sub>FT under cold equal-channel angular pressing and subsequent heating," *Metally*, No. 2, 28 – 35 (1994).
13. V. P. Mikryukov, Yu. F. Ivanov, and V. E. Gromov, *Physical Nature of Degradation of the Properties, Phase Composition and Defect Substructure of Reinforcing Steel under Long-Term Operation* [in Russian], SibGIU, Novokuznetsk (2007), 170 p.
14. Zh. G. Kovalevskaya, Yu. F. Ivanov, O. B. Perevalova, et al., "A study of the microstructure of surface layers of low-carbon steel after turning and ultrasonic finishing treatment," *Fiz. Met. Metalloved.*, **114**(1), 47 – 60 (2013).
15. V. E. Panin, L. S. Derevyagina, M. P. Lebedev, et al., "Scientific foundations of cold brittleness of structural steels with bcc crystal lattice and degradation of their structure in operation under negative temperatures," *Fiz. Mezomekh.*, **19**(2), 5 – 14 (2016).
16. L. I. Efron, *Metal Science in "Large" Metallurgy. Pipe Steels* [in Russian], Metallurgizdat, Moscow (2012), 696 p.
17. L. S. Derevyagina, N. M. Lemeshev, A. V. Korznikov, and S. V. Gladkovsky, "Effect of severe plastic deformation on the structure, mechanical properties and fracture behavior of low-carbon steel 12GBA," *AIP Conf. Proc.* (NY, USA), **1623**, 103 (2014).